PHILOSOPHICAL TRANSACTIONS OF THE ROYAL SOCIETY A MATHEMATICAL, PHYSICAL & ENGINEERING SCIENCES

The Resistance of Materials to Impact Erosion Damage

D. W. C. Baker, K. H. Jolliffe and D. Pearson

Phil. Trans. R. Soc. Lond. A 1966 **260**, 193-203
doi: 10.1098/rsta.1966.0043

XVI. The resistance of materials to impact erosion damage

By D. W. C. Baker,† K. H. Jolliffe‡ and D. Pearson§

† *South Eastern Region, R. and D. Department, C.E.G.B., Cockfosters, Barnet, Herts.*

‡ *Central Electricity Research Laboratories, C.E.G.B., Leatherhead*

§ *Marchwood Engineering Laboratories, C.E.G.B., Marchwood, Southampton*

[Plates 37 to 40]

The behaviour of established and potential turbine blade and erosion shield materials subject to impact erosion by water droplets of controlled size has been investigated over a range of impact velocities up to 1040 ft./s. Both the topographical form and the microstructural characteristics of damage have been studied, and correlated with the conditions of the test and the mechanical properties and phase constitution of the materials.

It has been found that the rate of erosion, as measured by mass loss, changes during the course of a test. An initial incubation period is generally followed, successively, by periods of increasing, constant, and then decreasing rates of erosion, possibly culminating in a second steady, but lower, rate of erosion. The rate of mass loss $(\partial M/\partial W)_{\text{max.}}$ during the initial steady period has been used as a measure of relative erosion resistance, and for a restricted range of materials it has been related to the impact velocity V and the angle of incidence θ by the expression

$$(\partial M/\partial W)_{\text{max.}} = K(V \sin\theta - V_c)^n \operatorname{cosec}\theta,$$

where K, V_c and n are constants characteristic of the material. This relation has been interpreted in terms of a fatigue mechanism of damage.

The investigation has shown that a number of materials are more resistant to erosion than either the cast cobalt-chromium alloy or the high speed tool steel currently used for erosion shields.

Introduction

In the final low pressure stages of steam turbines the rotor blades are subjected to erosion by steam-borne water droplets (Gardner 1964) and may suffer damage which disturbs their aerodynamic performance or jeopardizes their integrity. The progressive increase in size of turbines has intensified the problem because the longer blades required have greater tip speeds and therefore give rise to higher impact velocities.

In the investigations described here both the important engineering factors and the behaviour of materials have been studied with the aid of the erosion test rig installed at the Marchwood Engineering Laboratories (M.E.L.) of the C.E.G.B. The M.E.L. rig consists essentially of two rotor disks carried at each end of a common shaft and housed in separate sealed vacuum chambers. The shaft assembly is driven by a variable speed electric motor. The disks are provided with rim fittings for the attachment of holders carrying specimens of the materials under investigation. The impacting water is injected radially through a nozzle plate containing a row of small holes, and the natural breakup of the jets produces a uniform curtain of water droplets at one location in the circumferential path of the specimens. The impact conditions are, therefore, characterized by the random incidence of nominally spherical water drops over the whole face of the test

specimens. The droplet diameter can be varied in the range 350 to 1050 μm diameter by changing the size of the holes in the nozzle plate. The material evaluation tests described have been carried out, in the main, with a droplet size of 660 μm diameter, and under these conditions the amount of water striking a specimen at normal incidence during each revolution is estimated to be 3·6 mg/cm^2. In order to avoid jet interference effects at the high velocities used, only two specimens are mounted on each disk so that the curtain of water droplets is re-established between each passage. Tests have been carried out at impact velocities ranging from 465 ft./s to the maximum attainable, 1040 ft./s, and at angles of impact from 45° to 90° to the surface of the specimen. At the maximum impact velocity the number of passages of the specimen through the curtain of water droplets per hour is approximately $3{\cdot}3 \times 10^5$.

Various specimen designs have been used but the basic types shown in figure 1, plate 37, are suitable for most purposes. The two-piece specimen, figure 1 (*a*), was designed to avoid edge effects on the centre-piece in tests at impact angles other than normal. For tests at 90° incidence a one-piece version of the same dimensions may either be machined from the solid (1*b*) or the test material, in the form of a disk, may be brazed to the face of a backing piece made from a suitable steel (1*c*). The thickness of the head of the specimen is not critical and specimens up to 0·25 in. thick have been used for long-term tests.

The rig has generally been operated without direct control of the vacuum and the pressure in the chambers normally lies between 35 and 25 mmHg (abs.) (0·68 to 0·48 Lb./in.^{2} (abs.)) depending upon the ambient temperature.

Factors affecting rate of erosion

The progress of erosion has been followed by measuring the mass loss of the specimens at intervals and the results depicted by graphs of mass loss plotted against the number of passages through curtain of water droplets—for brevity referred to as 'number of impacts'. In order to compare tests carried out under different conditions, it is often more useful to express the loss of material by erosion as the 'loss in mass per unit area' and plot this against 'mass of water striking the specimen per unit area'; both presentations are of the same form and show four distinct regions as illustrated in figure 2: (i) an initial region, or incubation period, during which no significant loss in mass can be detected although changes in surface reflectivity may be observed; (ii) a region in which the rate of erosion increases steadily to (iii) a region in which the rate of erosion is at a maximum and sensibly constant which leads, ultimately, to (iv) a period in which the rate of erosion progressively diminishes, possibly again becoming constant, although this has yet to be proved conclusively in the M.E.L. tests.

It is noteworthy that in terms of practical significance, the level of mass loss obtaining when the latter parts of the curve are attained, say 250 to 400 mg/cm^2, is such that a real turbine blade would have sustained a serious amount of damage. For the purposes of comparative evaluation of materials the two parameters W_0 and $(\partial M/\partial W)_{\max.}$ defined in figure 2 have been used. The former, W_0, determined by extrapolation of the linear part of the curve to zero mass loss, is used because it is more readily determined than the termination of the incubation period. Generally, W_0 is approximately twice the value of the mass of water/unit area corresponding to the end of the incubation period.

Long duration tests were carried out at several impact velocities on specimens of a 12% chromium steel (En 56A, heat treated by oil quenching from 930 °C followed by tempering at 730 °C to give a hardness of 179–187 h.v.). The test results are depicted in figure 3; the parts of the curves representing the incubation and the bulk of the linear portions have been omitted for clarity.

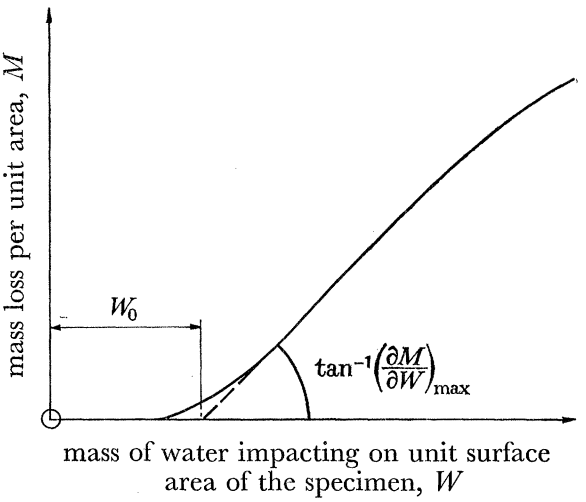

FIGURE 2. Typical erosion curve.

During these tests, the loss of thickness of the specimens was measured directly with respect to the position of the tips of the peaks of the eroded surface, and was also computed from the mass losses. The fact that the rate of change of these two parameters approached, but did not attain, equality indicates that the geometry of the specimen was continuously developing in the course of the tests.

Similar tests were carried out on the same material at three angles of the incidence: 45, 60 and 90° (i.e. normal to the surface). These tests were continued only to the end of the constant rate part of the test.

It appeared from these results that the maximum rate of erosion was not determined solely by the normal component of the impact velocity. However, a satisfactory correlation of the results obtained at all the angles of impact investigated was found to exist between $\sin\theta\,(\partial M/\partial W)_{\max.}$ and $(V\sin\theta)$, i.e. the following equation could be fitted to the data:

$$\sin\theta\left(\frac{\partial M}{\partial W}\right)_{\max.} = K(V\sin\theta - V_c)^n. \qquad (1)$$

The values of the arbitrary constants V_c and n were found to be 390 ft./s and 2·6 respectively. V_c is a parameter characteristic of the material, which may be interpreted physically as the value of the impact velocity below which erosion will not occur and in this sense it is analogous to the fatigue limit in fatigue tests.

On the basis that the quantity of water required to initiate erosion should be constant for a given normal component of impact velocity, an attempt was made to correlate W_0 and $V\sin\theta$. While a correlation was obtained it was less satisfactory than that of equation (1). As is to be expected the number of impacts required to initiate erosion diminishes as the normal impact velocity increases.

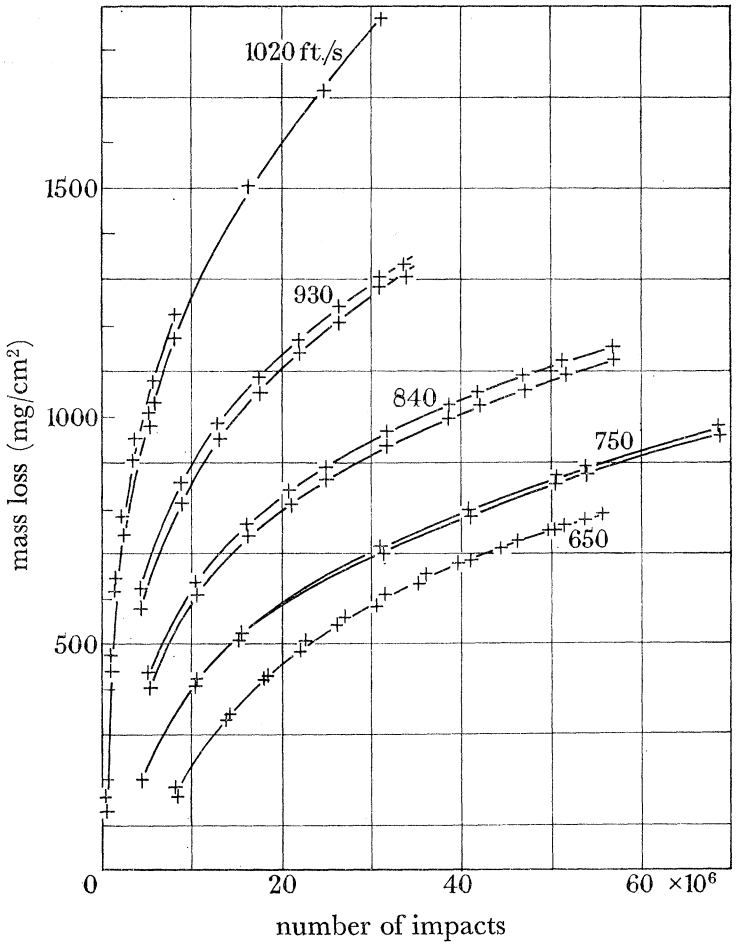

FIGURE 3. Effect of number of impacts and impact velocity on mass loss of En 56 at high mass losses.

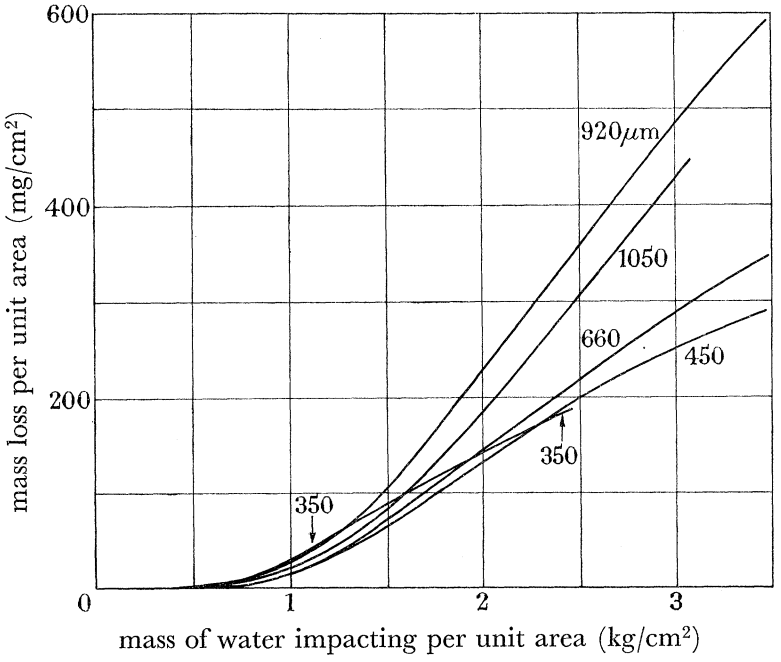

FIGURE 4. Typical erosion curves showing effect of drop diameter (impact velocity 1020 ft./s)

PHILOSOPHICAL TRANSACTIONS OF THE ROYAL SOCIETY A MATHEMATICAL, PHYSICAL & ENGINEERING SCIENCES

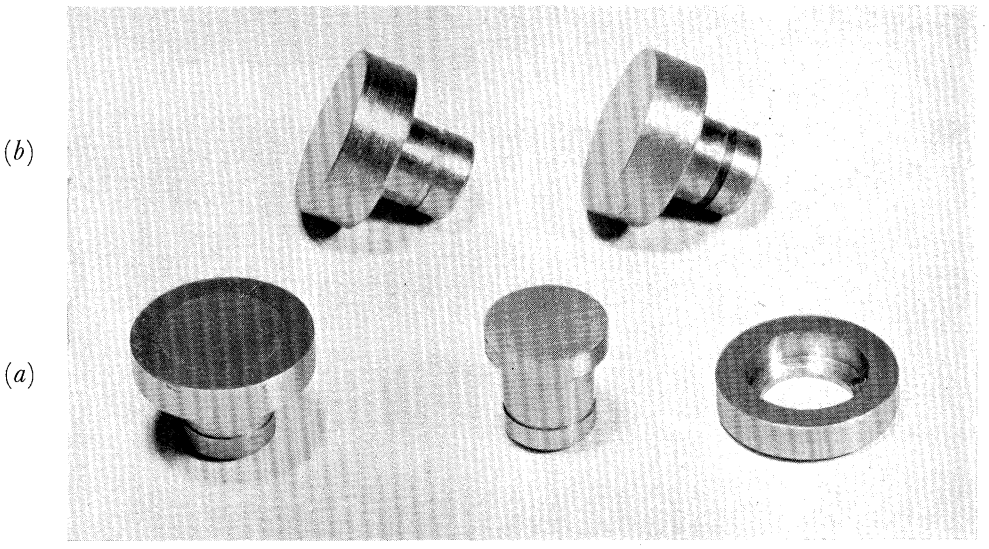

FIGURE 1. Types of erosion test specimen: (*a*) specimen with guard ring; (*b*) one-piece specimen; (*c*) brazed composite specimen.

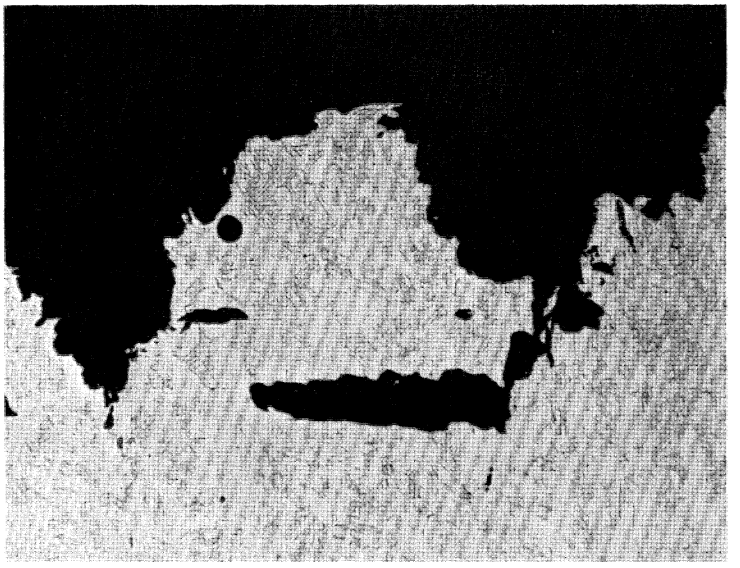

FIGURE 8. Cracking at base of pit in En 56 12 % chromium steel. (Magn. × 130.)

(*Facing p.* 196)

PHILOSOPHICAL TRANSACTIONS OF THE ROYAL SOCIETY A MATHEMATICAL, PHYSICAL & ENGINEERING SCIENCES

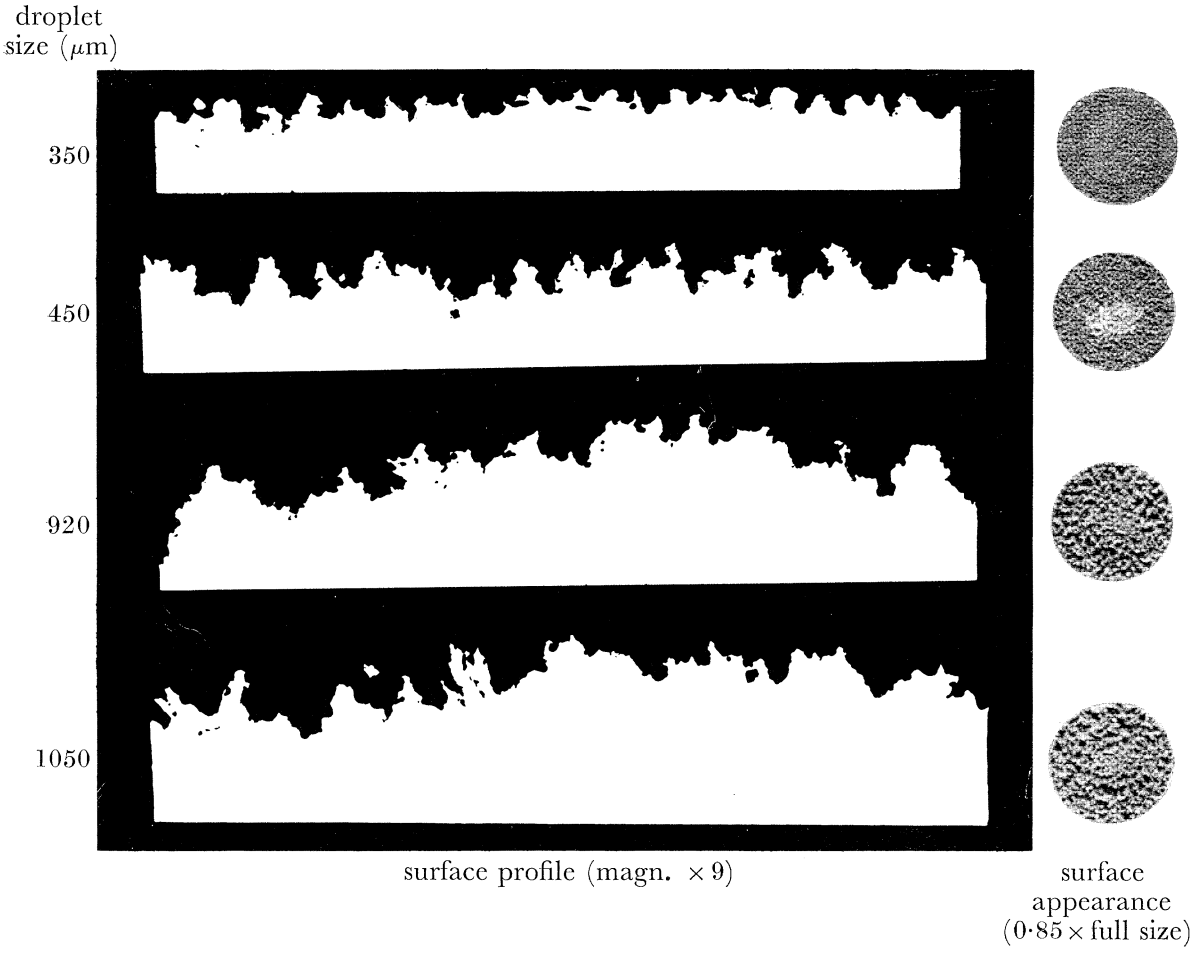

FIGURE 7. Effect of droplet size on the profile and surface appearance of eroded specimens.

PHILOSOPHICAL TRANSACTIONS OF THE ROYAL SOCIETY A MATHEMATICAL, PHYSICAL & ENGINEERING SCIENCES

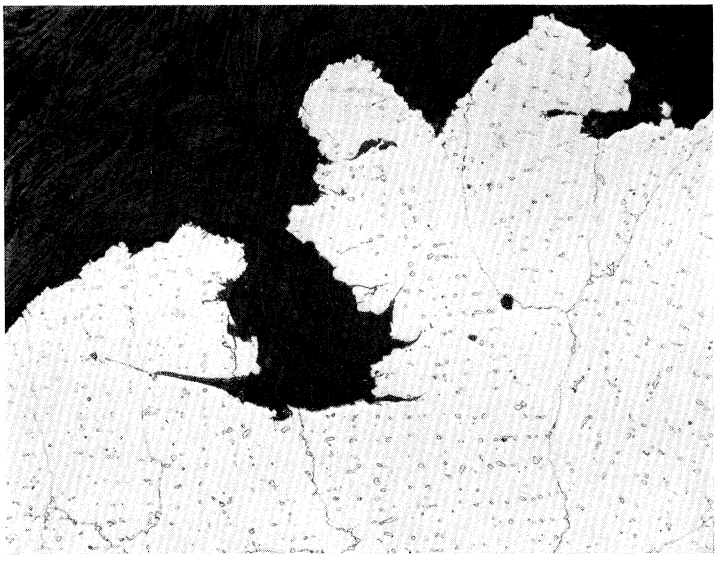

FIGURE 9. Form of cracking in peak remaining between erosion pits (cast no. 7 alloy). (Magn. × 110.)

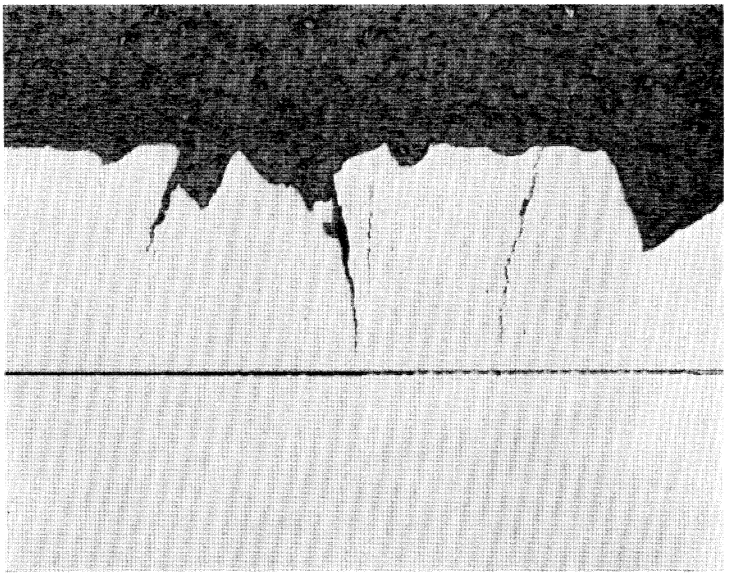

FIGURE 10. Cracking following macrostructure of cast cobalt–chromium alloy no. 1. (Magn. × 15.)

PHILOSOPHICAL TRANSACTIONS OF THE ROYAL SOCIETY A MATHEMATICAL, PHYSICAL & ENGINEERING SCIENCES

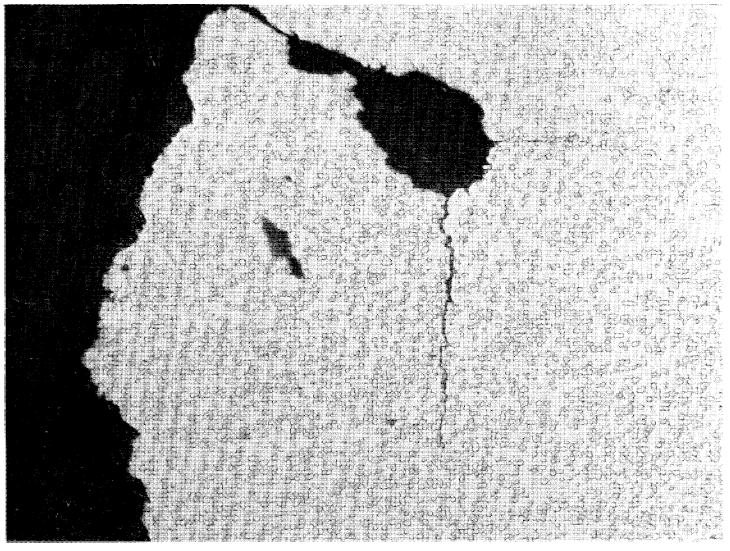

FIGURE 11. Cracking penetrating from the wall of an erosion pit in wrought cobalt–chromium alloy *W* 4. (Magn. × 190.)

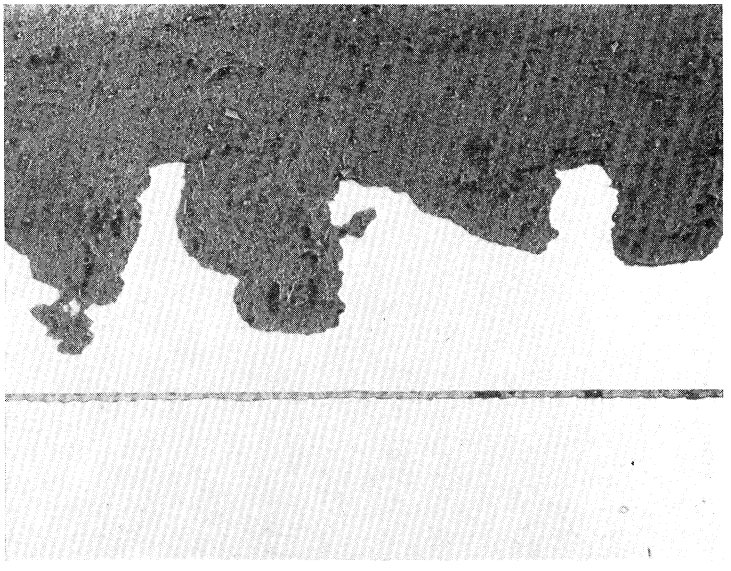

FIGURE 12. Form of erosion pitting in wrought cobalt–chromium alloy *W* 2. (Magn. × 15.)

PHILOSOPHICAL TRANSACTIONS OF THE ROYAL SOCIETY A MATHEMATICAL, PHYSICAL & ENGINEERING SCIENCES

The other major test parameter which has been investigated is the size of the impacting water droplets. Tests were carried out on the same 12% chromium steel at nominal droplet sizes ranging from 350 to 1050 μm diameter with the results shown in figure 4. Correlation with the parameter $(\partial M/\partial W)_{\max.}$ showed, in general, that the maximum rate of erosion increased with drop size (figure 5), although the results for tests with 920 and 1050 μm diameter droplets overlapped, possibly due to variations in other test

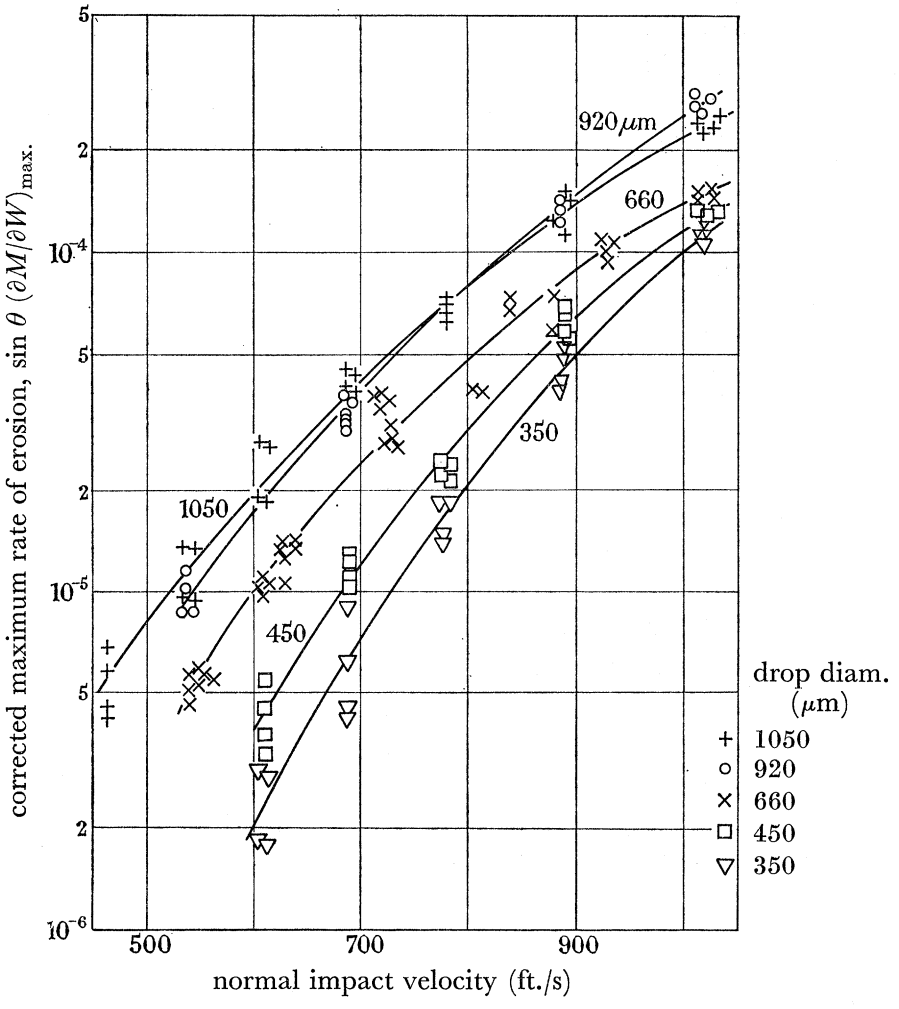

FIGURE 5. Effect of impact velocity and drop size on the maximum rate of erosion.

conditions. The effect of drop diameter appeared to be more marked the lower the impact velocity considered. There was evidence (figure 4) that the transition points marking the beginning and end of the linear portions of the curves are raised to higher levels of weight loss as the drop diameter increases. There was no evidence that these limits are affected by impact velocity.

EVALUATION OF MATERIALS FOR EROSION RESISTANT SHIELDS

In addition to the tests on En 56 steel, which were undertaken mainly to establish the significance of the various engineering parameters, the M.E.L. rig has been used to determine the resistance of established and potential blade erosion shield materials. At

present the inlet surface of blades in the later l.p. stages of modern British turbines are protected by shields of either a cast cobalt–chromium base alloy (1% C, 5% W, 26% Cr, Co) or of a wrought high speed tool steel (e.g. 0·7% C, 18% W, 6% Cr, Fe) heat treated, typically, to a hardness of 500 to 550 h.v. The shields are brazed in position using silver solders fusing in the range 620 to 650 °C. The resistance of both shield materials to erosion appears to be similar in practice although the hardness of the cobalt alloy is only 380 to 400 h.v. At the tip speeds now encountered in modern and future turbines neither material appears likely to provide an adequate life before replacement becomes necessary to preserve the underlying blade.

The established cast cobalt–chromium base alloy is one of a range of commercial alloys which have been devised to meet a variety of arduous service environments involving wear, erosion and corrosion at both low and elevated temperatures. Constitutionally these alloys consist of various carbides within cobalt-base solid solutions; the nature, morphology and relative proportions of these phases being modified by varying the carbon, chromium and tungsten contents.

In view of the lack of knowledge of the type of structure required for maximum resistance to impact erosion, it was considered that valuable information could be gained by correlating the erosion resistance to this range of alloys with their compositions, structures and other mechanical properties. Furthermore, since an erosion shield must not only withstand erosion but be able to accept the complex mechanical stresses arising both from its attachment to the blade and from the behaviour of the composite blade in service, it was important to evaluate the mechanical properties of potential shield materials. There is some evidence that materials possessing inadequate ductility may suffer cracking in service for reasons other than erosion. The minimum level of ductility required is difficult to assess because of the necessity of considering other physical properties such as the coefficient of thermal expansion and elastic moduli which vary from one material to another. Some guidance for alloys of similar constitution may be gained from the established cobalt–chromium shield alloy which offers a tensile elongation of about 1% and which has performed satisfactorily in service.

TABLE 1. DESIGNATION AND COMPOSITION OF CAST COBALT–CHROMIUM ALLOYS

alloy no.	C %	Co %	Cr %	W %	Fe %	Si %	Ni %	other elements
1	2·4	50·2	32·7	13·7	0·7	0·4	0·4	—
4	1·0	51·2	31·9	14·3	0·9	0·4	0·1	—
12	1·7	57·3	29·6	8·2	1·7	0·6	0·8	—
6	1·1	64·7	25·1	5·0	2·5	1·3	0·2	—
7	0·4	67·1	25·2	4·8	0·8	0·8	0·9	—
8	0·2	63·2	29·5	—	0·4	0·8	0·3	5·6% Mo

The designations and compositions of the cast alloys which were supplied by Deloro Stellite Ltd. are given in table 1. Samples of the alloys designated 7 and 8 were tested in both the 'as-cast' condition and after heat treatment at 1250 °C followed by water quenching in an effort to raise the amount of carbon in solid solution and minimize the amount of brittle carbide phase in the structure.

The alloys were all prepared in the form of precision cast disks about 0·080 in. thick and

were brazed to backing pieces as described earlier. The erosion tests were carried out using water droplets of 660 μm diameter and an impact velocity of 1020 ft./s and were continued to the point where the rate of erosion began to deviate from the maximum rate linear portion of the curve. Typical results are shown in figure 6. The results of hardness determinations and tensile and fatigue tests carried out on precision cast bars from the same melts

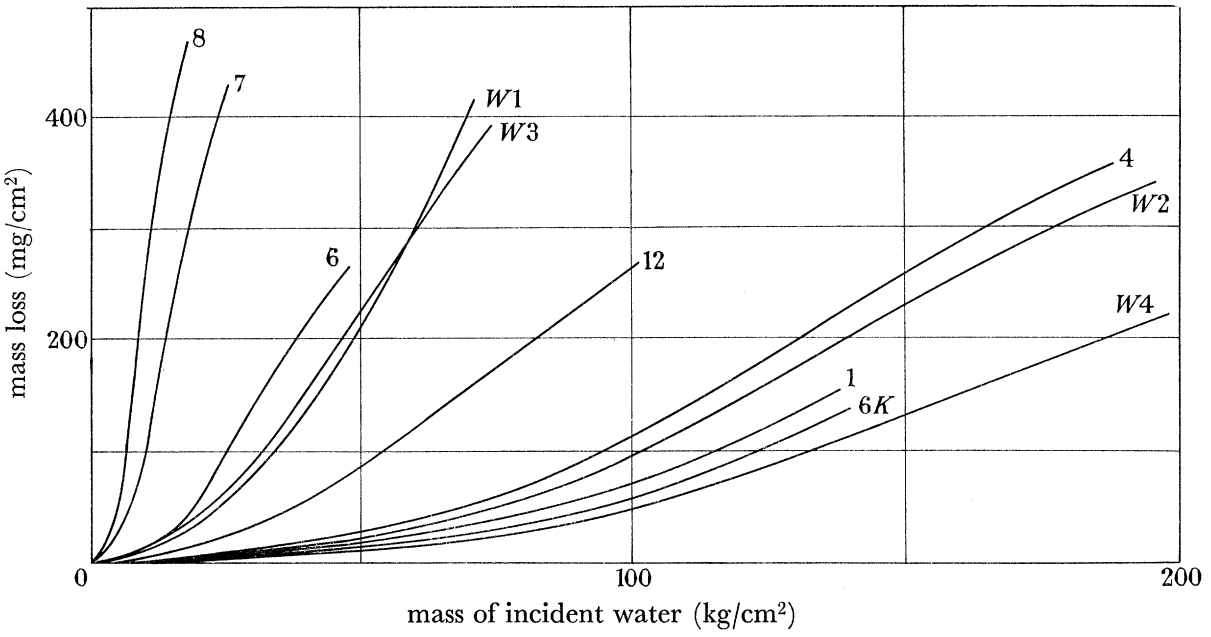

FIGURE 6. Typical erosion curves for cobalt–chromium base alloys.

TABLE 2. MECHANICAL PROPERTIES AND EROSION WEIGHT LOSS MEASUREMENTS OF CAST COBALT–CHROMIUM BASE ALLOYS

alloy no.	hardness (h.v.)	u.t.s. (tons/in.^{2})	fatigue strength (tons/in.^{2} (10^6 cycles))	maximum rate of mass loss (mg/cm^2 h)
1	568	40·0	17·5	2·6
4	552	62·0	37·5	3·4
12	509	57·8	27·0	4·0
6	407	59·0	29·0	8·3
7	333	54·0	22·5	26·8
7, heat treated	296	50·6	20·0	28·6
8	345	53·5	24·0	47·1
8, heat treated	306	46·4	25·0	35·8

are recorded in table 2 together with erosion rate data. The best correlation of the maximum rates of erosion was obtained with hardness. The correlations between erosion rate and the tensile fatigue strength values were less satisfactory, particularly in the case of the composition designated alloy 1. In this instance, however, it is noteworthy that the material is very brittle and the tensile and fatigue results need to be treated with caution since the alloy is likely to be very sensitive to effects such as non-axiality of loading and surface imperfections.

The lower carbon content alloys (7 and 8) in both the 'as cast' and 'heat-treated' condition offered lower resistance to erosion than the established alloy. The high temperature solution heat treatment appeared to soften the alloys but not affect their erosion resistance significantly. The alloys containing greater quantities of carbon exhibited higher resistance to erosion in the order 12, 4, 1. The ductility of the latter group, certainly of alloys 4 and 1, is probably inadequate and it is doubtful whether practical advantage can be taken of their greater erosion resistance in the particular application of interest here.

The metallographic observations made on these alloys, which are described later, together with the theoretical view that erosion is a fatigue phenomenon stimulated interest in the possibility of improving the properties of this type of alloy by modifying the structure by hot working. Two approaches appeared feasible, either to improve the erosion resistance without necessarily improving the other relevant mechanical properties or to improve the mechanical properties to a tolerable level in alloys which appear to have better erosion resistance compared with the established alloy.

TABLE 3. DESIGNATION, COMPOSITION AND TYPICAL MECHANICAL PROPERTIES OF WROUGHT COBALT–CHROMIUM BASE ALLOYS

alloy designation	composition (%) (balance Co)							u.t.s. (tons/in.^{2})	elongation (%)	hardness (h.v.)
	C	Cr	W	Si	Mn	Ni	Fe			
*W*1	1·03	29·0	5·03	0·62	0·62	0·65	1·2	79	7·0	455
*W*2	1·72	29·5	4·96	0·61	0·66	0·65	0·42	78	2·5	480
*W*3	0·71	30·5	7·20	0·97	0·66	0·60	0·48	79	6·0	430
*W*4	1·18	30·3	9·02	0·19	0·55	0·55	0·38	82	2·0	506
6*B*	1·1	30	4·5	(nominal composition)				—	—	400
6*K*	1·6	31	4·5	(nominal composition)				—	—	520

Two wrought alloys of the composition designated 6*B* and 6*K* in table 3 were commercially available in small quantities and these were supplemented by four experimental wrought alloys designed to evaluate the effect of tunsgten and carbon contents in a given 30% chromium–cobalt base (alloys *W*1, *W*2, *W*3 and *W*4 in table 3). The latter samples were produced from $2\frac{1}{2}$ in. square ingots forged to $\frac{5}{8}$ in. thick slab at about 1230 °C and rolled at the same temperature to 0·080 in. thick sheet followed by heat treatment at 1230 °C and water quenching. Hardness values were determined on all the samples and tensile tests carried out on the experimental alloys. Fatigue tests have not yet been conducted. The available information is given in table 3.

Erosion tests were again carried out with water droplets of 660 μm diameter and at impact velocity of 1020 ft./s and typical results are plotted in figure 6.

The wrought alloys 6*B* and *W*1, both containing about 1% C and 5% W exhibited a similar level of erosion resistance to the cast 6 version of comparable composition. Thus, the fact that the material has been worked and the structure refined does not necessarily give in itself, a higher erosion resistance under these test conditions, although the ductility and strength are substantially improved. The lower-carbon but higher-tungsten wrought alloy *W*3 (0·5% C and 9% W) also exhibited similar properties to cast 6 material.

On the other hand, the wrought alloys *W*2, *W*4 and 6*K*, although less highly alloyed than the cast 12, 1 and 4 alloys, exhibited resistances at least comparable to the best of them, coupled with a ductility equal or better than that of the cast 6 alloy.

PHILOSOPHICAL TRANSACTIONS OF THE ROYAL SOCIETY A MATHEMATICAL, PHYSICAL & ENGINEERING SCIENCES

On the basis of these results, it appears that hot working may, or may not, have a beneficial influence depending upon the circumstances. If the ductility is adequate, for a given erosion regime, further enhancement of this property by hot working does not improve the erosion resistance, but for alloys with very limited ductility in the cast state, e.g. alloys like 12, 4 and 1, working appears to improve ductility and give a concommitant gain in erosion resistance.

In pursuing the premise that erosion resistance and fatigue strength are intimately related, tests have also been carried out on a 5% chromium alloy die steel which had been subjected to the thermomechanical treatment known as ausforming (Schmatz & Zackay 1959) to develop a very high tensile strength coupled with an unusually high fatigue strength/u.t.s. ratio. The properties of the material are summarized in table 4.

TABLE 4. MECHANICAL PROPERTIES OF AUSFORMED STEEL

(Nominal composition: 0·4% C, 5% Cr, 1·3% Mo, 1% V, 1·1% Si.)

hardness	775 h.v.
ultimate tensile strength	202 tons/in.^{2}
elongation (2 in. gauge length)	5%
reduction of area	33%
impact value (Charpy)	10 ft. Lb.
fatigue strength	0 ± 70 tons/in.^{2}: unbroken after 10^7 cycles
	0 ± 80 tons/in.^{2}: (i) broken $4{\cdot}7 \times 10^5$ cycles
	(ii) broken $7{\cdot}6 \times 10^5$ cycles

The only test yet completed on the ausformed steel, carried out at 1040 ft./s and with droplets of 750 μm diameter, was of relatively short duration but it appeared to be more resistant to erosion than any of the other alloys tested.

TOPOGRAPHICAL FEATURES OF EROSION DAMAGE

The appearance and surface profile of the 12% chromium steel specimens eroded in the variable drop size tests described above are illustrated in figure 7, plate 38. In general, the topographical examination showed the following features:

(*a*) The average distance between adjacent peaks in the surface increases as the mass loss increases: this is probably associated with the intersection of widening pits which tends to eliminate, progressively, the narrowest of the escarpments remaining between them.

(*b*) Within the duration of the longest tests carried out, the average depth of the erosion pits continually increases.

(*c*) There is no observable topographical difference between specimens which have suffered the same mass loss produced by water droplets of the same size but different impact velocities.

(*d*) For corresponding positions on the curves of mass loss against mass of impacting water the coarseness of the surface increases with drop size and the distance between adjacent erosion peaks is proportional to, and of the same order as, the droplet diameter.

PHILOSOPHICAL TRANSACTIONS OF THE ROYAL SOCIETY A MATHEMATICAL, PHYSICAL & ENGINEERING SCIENCES

Structural aspects of erosion damage

Metallographic examination of the 12% chromium steel samples indicated that erosion progressed by the intersection of cracks and detachment of discrete fragments of material. There was evidence that cracks are initiated both at the original surface of the specimen and from the walls and bases of erosion pits. In rare instances fissures were observed parallel to the original surface but beneath the base of an erosion pit. This is illustrated in figure 8, plate 37, where the fissure has developed and met, or propagated as, a vertical crack. Apparently, isolated fissures have been observed, but it is difficult to be certain that they do not communicate with the surface in another plane. However, the possibility that subsurface cracks may be formed cannot be neglected. In detail, the cracks tended to be fine and branched and reminiscent of corrosion fatigue failures in this type of material.

The two cast cobalt–chromium alloys, designated 7 and 8, which contain less than 0·5% carbon, consisted of relatively large cored grains of solid solution containing isolated carbide particles about 10 μm in size and discontinuous films or strings of finer particles at the grain boundaries. Macroscopically the erosion took the form of relatively wide-mouthed pits which had tended to overlap in places. Many intercrystalline cracks were visible in the remaining material and these showed no preference to pass through, or around the interface of, the carbide particles. As in the 12% chromium steel a number of subsurface fissures were observed. Typical cracking in one of the peaks between the pits is illustrated in figure 9, plate 39.

In the alloy designated no. 6 which contained a greater quantity of carbon (1%), the interdendritic eutectiferous carbide areas were almost continuous. Few cracks were observed in the residual material but there was evidence that they tended to follow the carbide-rich areas. The pits were relatively deep and often showed near-vertical sides.

The alloys designated 1, 4 and 12 contained even greater quantities of carbide and the tendency of the cracks to run through these brittle areas became particularly marked. The no. 1 alloy had a pronounced columnar structure and many long cracks penetrated from the surface through the full thickness of the specimen without intersecting. Thus, if the structure had been less directional, the cracks would probably have had a greater opportunity to intersect and the loss of material would have been considerably greater. A typical area is shown in figure 10, plate 39.

The observations made on the more highly alloyed cast alloys suggested that while they possessed greater erosion resistance, the cracks which did form tended to propogate through the relatively brittle carbide phases. This led to the belief that the resistance to cracking and erosion might be improved by refinement of the structure and destruction of the continuity of the carbide phases. The extent to which this was achieved by hot working is illustrated by the structure, figure 11, plate 40, of the experimental wrought alloy *W*4. The interdendritic carbides have been broken down into a fairly homogeneous dispersion of particles about 1 to 10 μm in diameter, and the grain size reduced to about 10 to 20 μm diameter.

The macroscopic form of the pitting damage in the wrought alloys, figure 12, plate 40, was very similar to that of the cast specimens. Only a few cracks were observed and these tended to be short in length and to follow random paths through the structure as shown in figure 11.

PHILOSOPHICAL TRANSACTIONS OF THE ROYAL SOCIETY A MATHEMATICAL, PHYSICAL & ENGINEERING SCIENCES

Microhardness measurements made on the matrices of the cast alloys indicated that their hardness was raised by only relatively small amounts, from about 430 h.v. for the alloys 7 and 8, to about 460 h.v. for alloy 1. Even this apparent increase may be attributable to a progressively higher concentration of very fine carbide particles in the matrix as the alloying content is raised. There was some evidence that the hardness of the matrix was significantly increased (by up to 40 h.v.) close to any remaining surface of a test piece and near the surfaces of the erosion pits. This increase is consistent with the view that the impact of water droplets work hardens the material and the cyclic nature of the stressing ultimately leads to fatigue failure. Microhardness surveys to determine the detailed distribution and depth of this hardening have not yet been completed. It has not proved possible to make microhardness measurements on the more erosion resistant wrought alloys with the same freedom because of the close spacing of the carbide particles, but such measurements as have been made suggest that their hardnesses are similar to those of the cast alloys.

General comments

The work completed so far has provided a good understanding of the significance of the various engineering factors governing erosion. The nature of the erosion damage produced in the M.E.L. rig suggests that fatigue cracks are generated by the repeated impact of the water droplets and that these ultimately intersect to release discrete fragments of material.

The study of materials has been confined largely to commercially available and experimental cobalt–chromium base alloys in both cast and wrought form. These constitutionally complex alloys are of immediate interest for erosion shields but investigation of simpler alloys is also required in order to gain a better understanding of the mechanism of erosion. In the more highly alloyed cast materials, it has been found that cracking tends to pass through the continuous carbide phases present in the structure. Hot working provides one means by which the continuity of carbide phase can be eliminated. It has been shown that wrought alloys possessing better erosion resistance than the established cast shield material and better mechanical properties than cast alloys of comparable erosion resistance, may be devised. There is every reason to believe that the nature, size and distribution of the carbide phases may be optimized and the erosion resistance improved still further.

The excellent erosion resistance of the ausformed steel may be exploited if means can be found for attaching shields of such high-strength steels to turbine blades without causing over-tempering and loss of strength. Alternatively it may be possible to harden locally those parts of a turbine blade that suffer erosion damage; this would involve a careful choice of steel and thermomechanical treatment.

The authors would like to acknowledge the assistance of many members of the staff of their respective establishments. They would also like to express their thanks to the Central Electricity Generating Board for permission to publish this paper.

References (Baker, Jolliffe & Pearson)

Gardner, G. C. 1964 *Proc. Inst. Mach. Engrs*, **178**, 1, no. 23.
Schmatz, D. J. & Zackay, V. F. 1959 *Trans. Am. Soc. Metals*, **51**, 476.

PHILOSOPHICAL TRANSACTIONS OF THE ROYAL SOCIETY A MATHEMATICAL, PHYSICAL & ENGINEERING SCIENCES

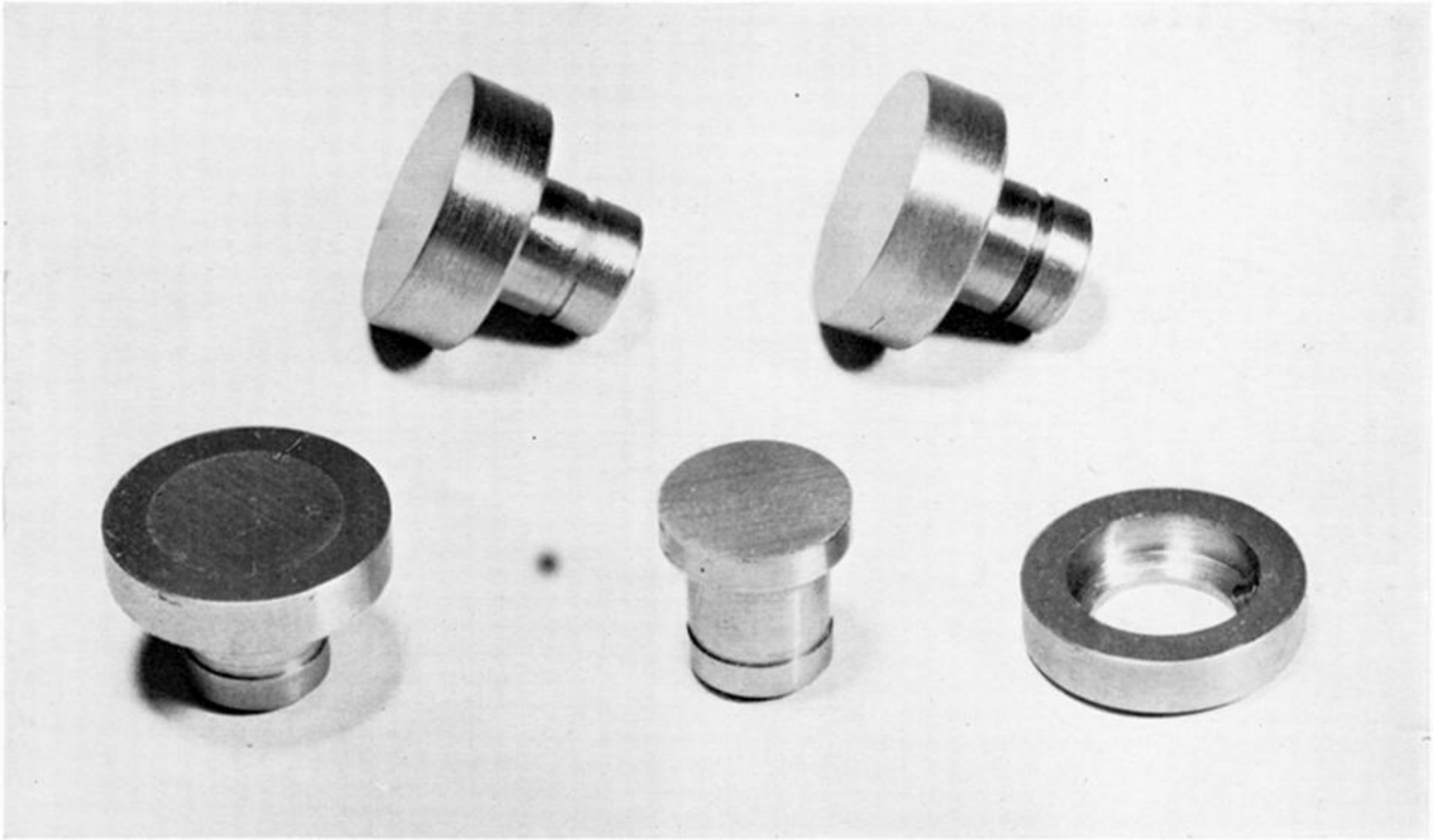

FIGURE 1. Types of erosion test specimen: (*a*) specimen with guard ring; (*b*) one-piece specimen; (*c*) brazed composite specimen.

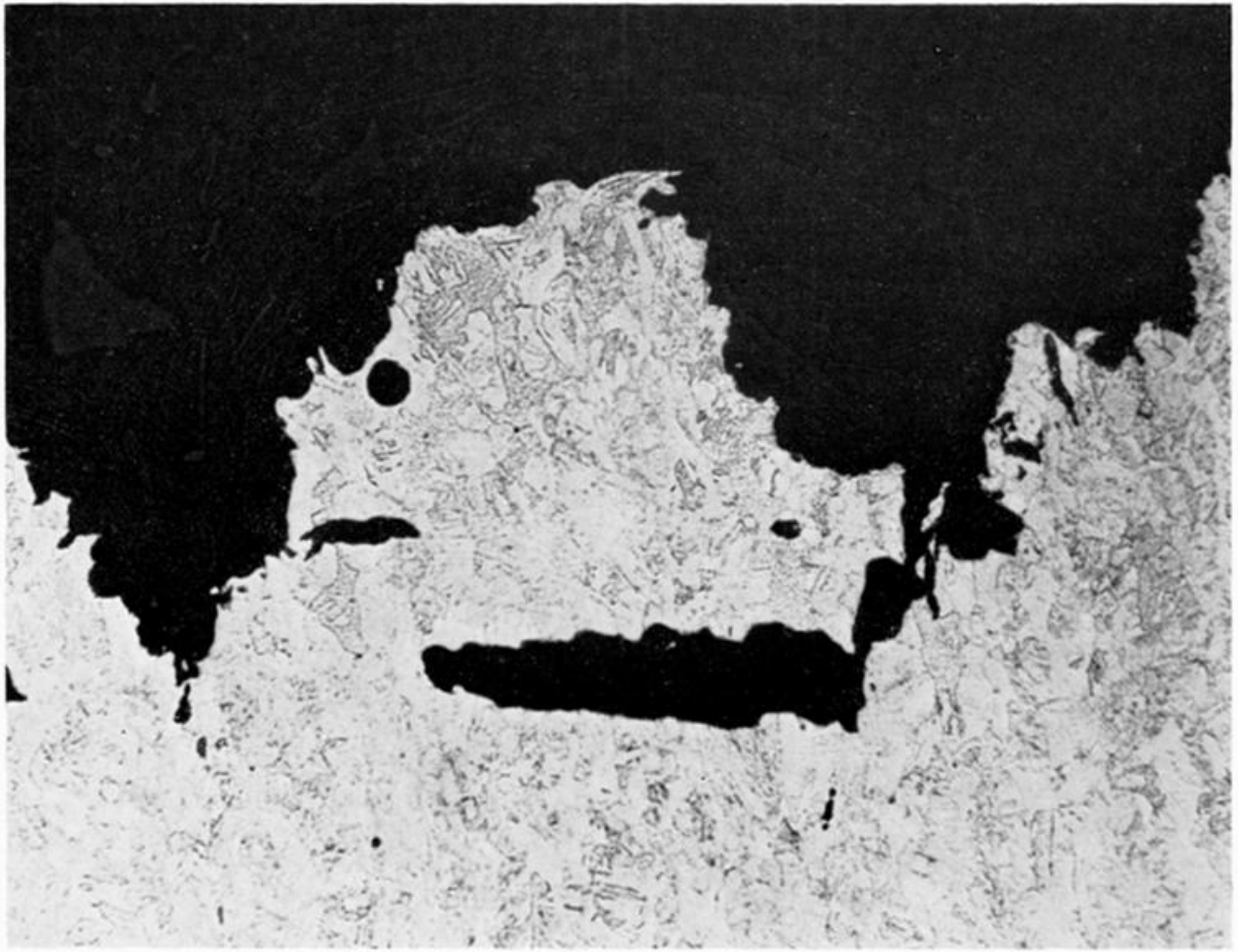

FIGURE 8. Cracking at base of pit in En56 12% chromium steel. (Magn. ×130.)

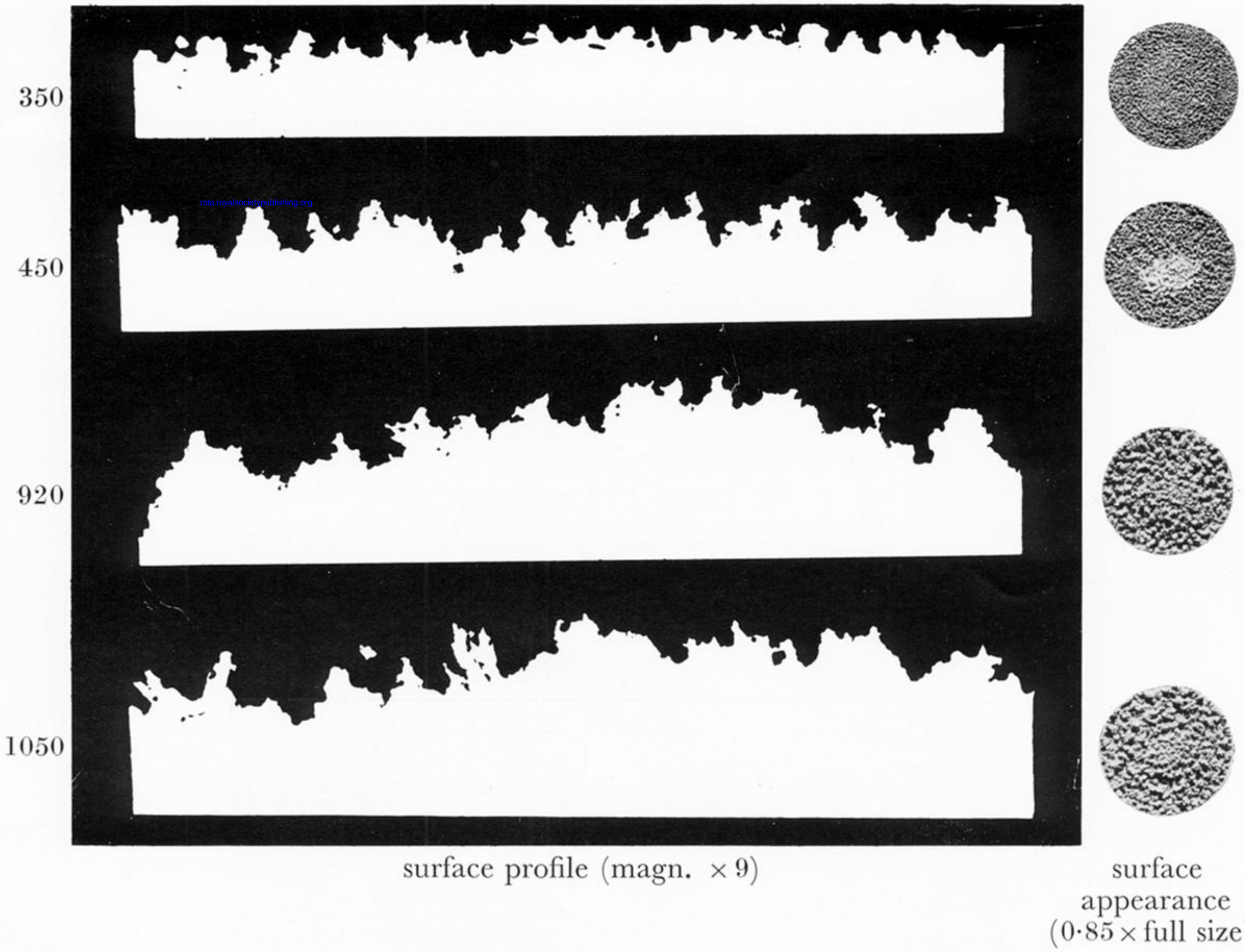

PHILOSOPHICAL TRANSACTIONS OF THE ROYAL SOCIETY A MATHEMATICAL, PHYSICAL & ENGINEERING SCIENCES

FIGURE 7. Effect of droplet size on the profile and surface appearance of eroded specimens.

IGURE 9. Form of cracking in peak remaining between erosion pits (cast no. 7 alloy). (Magn. ×110.)

PHILOSOPHICAL TRANSACTIONS OF THE ROYAL SOCIETY A MATHEMATICAL, PHYSICAL & ENGINEERING SCIENCES

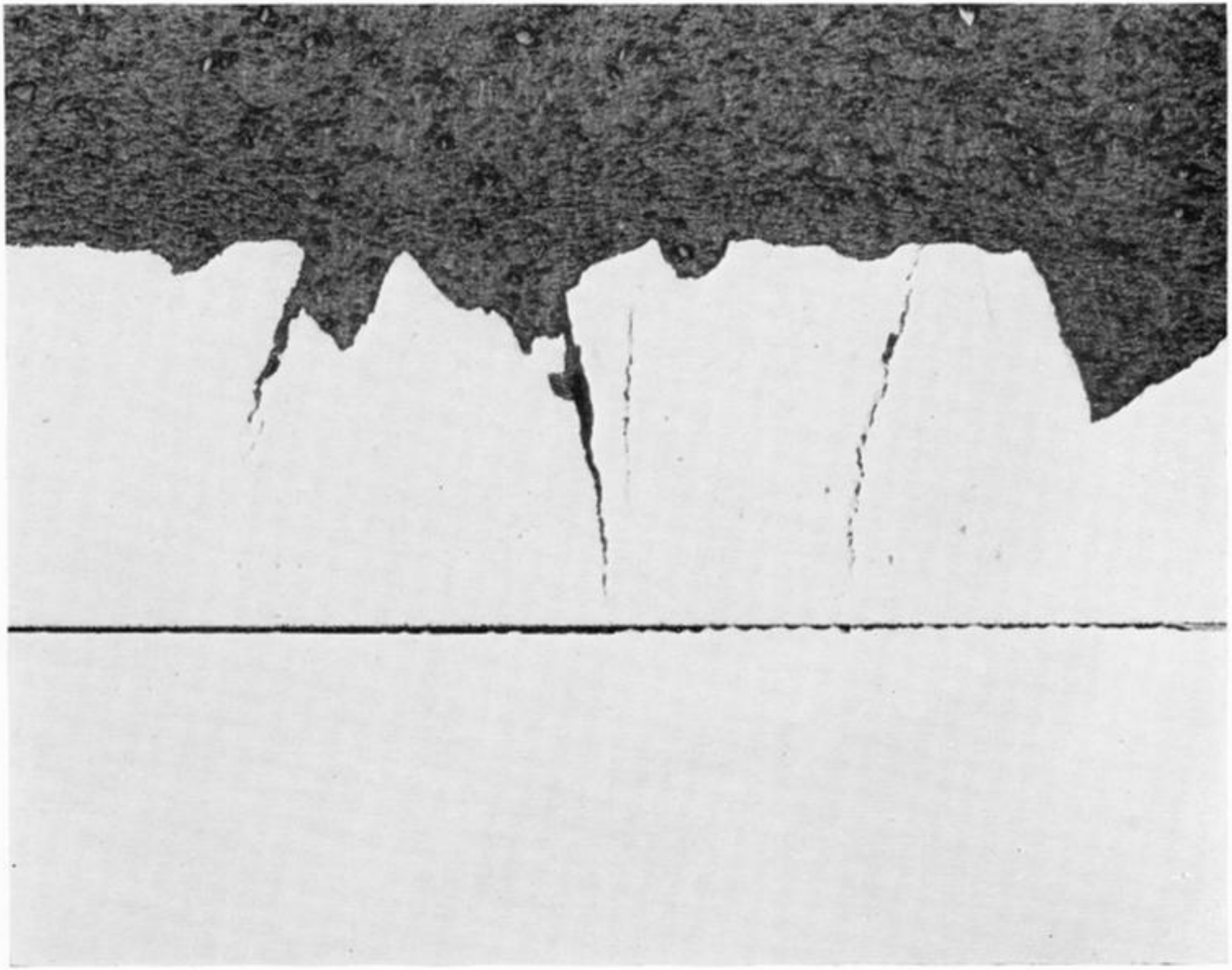

FIGURE 10. Cracking following macrostructure of cast cobalt–chromium alloy no. 1. (Magn. × 15.)

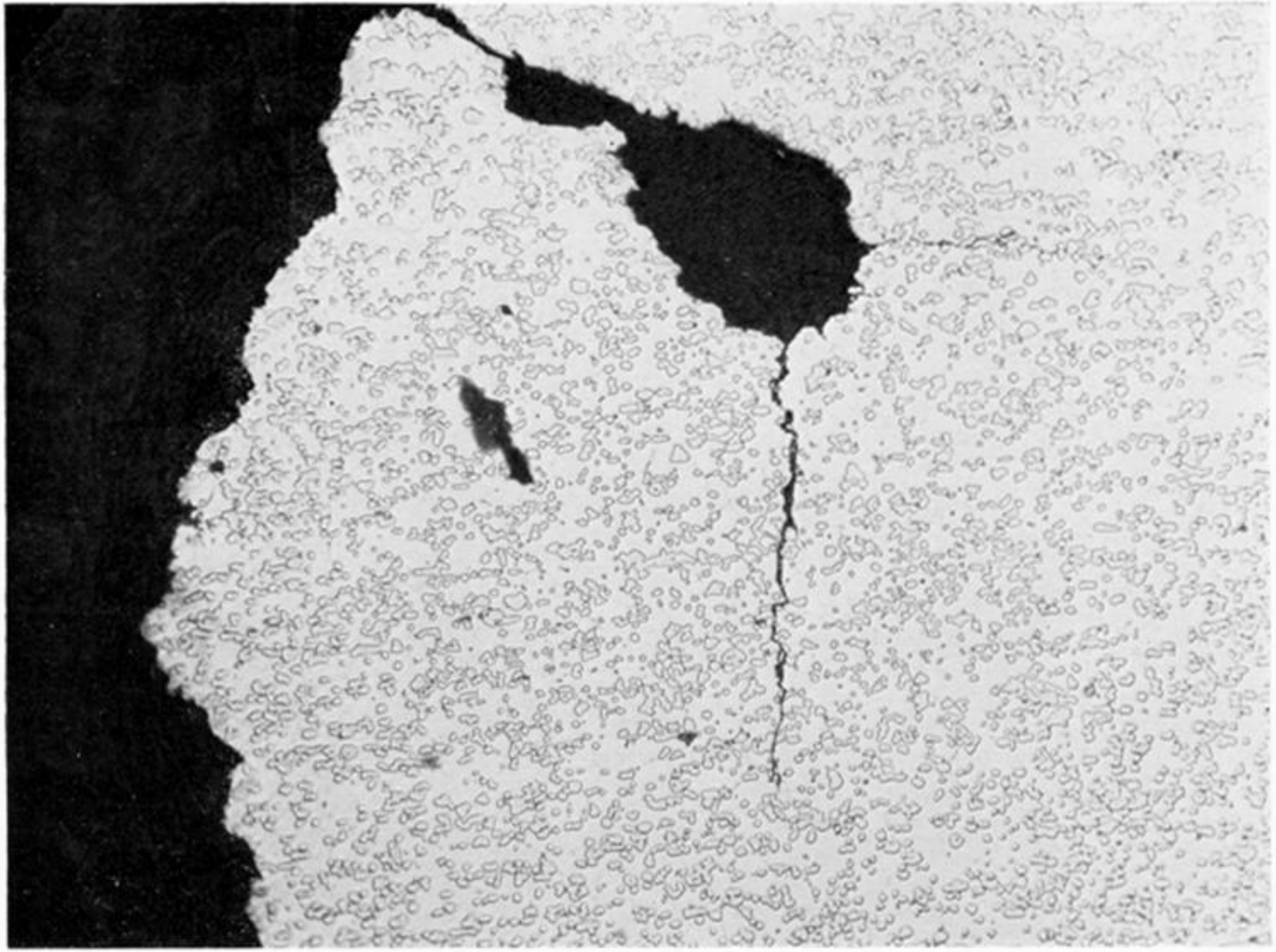

IGURE 11. Cracking penetrating from the wall of an erosion pit in wrought cobalt–chromium alloy *W* 4. (Magn. × 190.)

PHILOSOPHICAL TRANSACTIONS OF THE ROYAL SOCIETY A MATHEMATICAL, PHYSICAL & ENGINEERING SCIENCES

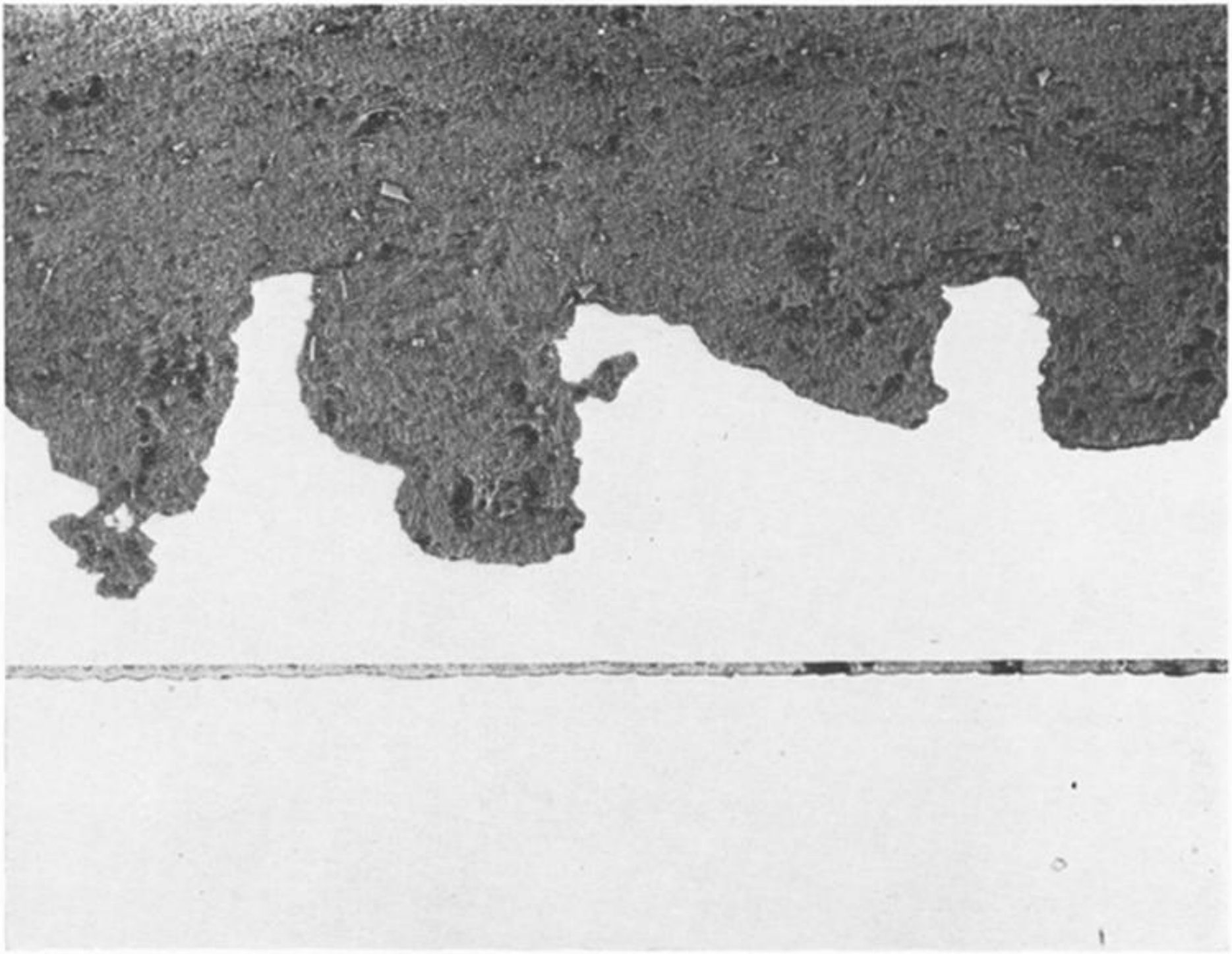

IGURE 12. Form of erosion pitting in wrought cobalt–chromium alloy *W* 2. (Magn. × 15.)

PHILOSOPHICAL TRANSACTIONS OF THE ROYAL SOCIETY A MATHEMATICAL, PHYSICAL & ENGINEERING SCIENCES